nature physics

SUPPLEMENTARY INFORMATION

DOI: 10.1038/NPHYS4118

In the format provided by the authors and unedited.

Proposal for gravitational-wave detection beyond the standard quantum limit through EPR entanglement

Yiqiu Ma,[1] Haixing Miao,[2] Belinda Heyun Pang,[1] Matthew Evans,[3]
Chunnong Zhao,[4] Jan Harms,[5,6] Roman Schnabel,[7] and Yanbei Chen[1]

[1] *Theoretical Astrophysics 350-17, California Institute of Technology, Pasadena, CA 91125, USA*
[2] *School of Physics and Astronomy, University of Birmingham, Birmingham, B15 2TT, United Kingdom*
[3] *Massachusetts Institute of Technology, Cambridge, Massachusetts 02139, USA*
[4] *School of Physics, University of Western Australia, Western Australia 6009, Australia*
[5] *Università degli Studi di Urbino "Carlo Bo", I-61029 Urbino, Italy*
[6] *INFN, Sezione di Firenze, Firenze 50019, Italy*
[7] *Institut für Laserphysik and Zentrum für Optische Quantentechnologien, Universität Hamburg, Luruper Chaussee 149, 22761 Hamburg, Germany*

(Dated: March 15, 2017)

This is a supplementary material for the paper: "Proposal for Gravitational-Wave Detection Beyond the Standard Quantum Limit using EPR Entanglement". The purpose of this material is to present the details about (1) the derivation of the sensitivity formula; (2) the choice of system parameters; (3) the effect of loss;

I. DERIVATION OF THE SENSITIVITY FORMULA

First, for each audio-sideband frequency Ω, the field input-output relations of the squeezer (the pumped OPA) can be written as:

$$\begin{aligned}
&\hat{a}(\omega_0+\Omega)=\mu\hat{a}_{\rm in}(\omega_0+\Omega)+\nu\hat{b}^\dagger_{\rm in}(\omega_0+\Delta-\Omega),\quad \hat{b}(\omega_0+\Delta+\Omega)=\mu\hat{b}_{\rm in}(\omega_0+\Delta+\Omega)+\nu\hat{a}^\dagger_{\rm in}(\omega_0-\Omega);\\
&\hat{a}^\dagger(\omega_0-\Omega)=\mu^*\hat{a}^\dagger_{\rm in}(\omega_0-\Omega)+\nu^*\hat{b}_{\rm in}(\omega_0+\Delta+\Omega),\quad \hat{b}^\dagger(\omega_0+\Delta-\Omega)=\mu^*\hat{b}^\dagger_{\rm in}(\omega_0+\Delta-\Omega)+\nu^*\hat{a}_{\rm in}(\omega_0+\Omega),
\end{aligned}\tag{1}$$

where $\hat{a}$ and $\hat{b}$ describe the generated signal and idler fields near ω_0 and $\omega_0\pm\Delta$, respectively. The fields $\hat{a}_{\rm in},\hat{b}_{\rm in}$ represent the vacuum fields entering into the squeezer. The phenomenological coefficient μ and ν are determined by the $\chi^{(2)}-$nonlinearity coefficient of the crystal and the pumping field strength [1]. Field commutation relation requires them to satisfy the relation $|\mu|^2-|\nu|^2=1$. Since the phase of μ and ν can be absorbed into the definition of creation and annihilation operators, we can parametrise them as $\mu=\cosh r$ and $\nu=\sinh r$, where r is usually denoted to be the squeezing degree of the OPA. In the so-called two-photon formalism where we define:

$$\begin{aligned}
\hat{a}_1(\Omega)&=\frac{\hat{a}(\omega_0+\Omega)+\hat{a}^\dagger(\omega_0-\Omega)}{\sqrt{2}},\quad \hat{b}_1(\Omega)=\frac{\hat{b}(\omega_0+\Delta+\Omega)+\hat{b}^\dagger(\omega_0+\Delta-\Omega)}{\sqrt{2}};\\
\hat{a}_2(\Omega)&=\frac{\hat{a}(\omega_0+\Omega)-\hat{a}^\dagger(\omega_0-\Omega)}{\sqrt{2}i},\quad \hat{b}_2(\Omega)=\frac{\hat{b}(\omega_0+\Delta+\Omega)-\hat{b}^\dagger(\omega_0+\Delta-\Omega)}{\sqrt{2}i},
\end{aligned}\tag{2}$$

the relations in Eq. (1) then can be represented in another form (in the following, $\hat{a}_{1,2}(\Omega)$ and $\hat{b}_{1,2}(\Omega)$ will be simply written as $\hat{a}_{1,2}$ and $\hat{b}_{1,2}$):

$$\hat{a}_1+\hat{b}_1=e^r(\hat{a}_{\rm in1}+\hat{b}_{\rm in1}),\quad \hat{a}_1-\hat{b}_1=e^{-r}(\hat{a}_{\rm in1}-\hat{b}_{\rm in1});\tag{3}$$

$$\hat{a}_2+\hat{b}_2=e^{-r}(\hat{a}_{\rm in2}+\hat{b}_{\rm in2}),\quad \hat{a}_2-\hat{b}_2=e^{r}(\hat{a}_{\rm in2}-\hat{b}_{\rm in2}),\tag{4}$$

(the $\hat{a}_{\rm in1,2},\hat{b}_{\rm in1,2}$ are defined in the same way as Eq. (2)). EPR-type commutation relation $[\hat{a}_1-\hat{b}_1,\hat{a}_2+\hat{b}_2]=0$ allows the existence of the state in which the fluctuations of quadrature combinations $(\hat{a}_1-\hat{b}_1)/\sqrt{2}$ and $(\hat{a}_2+\hat{b}_2)/\sqrt{2}$ are much below the vacuum level. Therefore $\hat{b}_1$ is correlated with $\hat{a}_1$ while $\hat{b}_2$ is correlated with $-\hat{a}_2$, and further more $\hat{a}_{-\theta}=\hat{a}_1\cos\theta-\hat{a}_2\sin\theta$ correlates with $\hat{b}_\theta=\hat{b}_1\cos\theta+\hat{b}_2\sin\theta$. Using homodyne detection scheme, $\hat{a}_{-\theta}$ and $\hat{b}_\theta$ can be measured. When we do conditioning by processing these measurement results, we assume the measurement result of the idler field quadrature $\hat{b}_\theta$ is filtered with a filtering gain factor g and then combined with the signal field quadrature $\hat{a}_{-\theta}$, leads to:

$$\hat{a}^g_{-\theta}=\hat{a}_{-\theta}-g\hat{b}_\theta=(\hat{a}_1-g\hat{b}_1)\cos\theta-(\hat{a}_2+g\hat{b}_2)\sin\theta.\tag{5}$$

It is easy to show that the spectrum of $\hat{a}^g_{-\theta}$ is:

$$S_{\hat{a}^g_{-\theta}\hat{a}^g_{-\theta}} = (\mu - g\nu)^2 + (\nu - g\mu)^2. \tag{6}$$

For realising an optimal filtering (which is the so-called "Wiener filtering") so that $S_{\hat{a}^g_{-\theta}\hat{a}^g_{-\theta}}$ takes its minimum value, we can solve $\delta S_{\hat{a}^g_{-\theta}\hat{a}^g_{-\theta}}/\delta g = 0$, which leads to the Wiener filter gain factor $g_{\rm opt}$ and conditional squeezing spectrum:

$$g_{\rm opt} = \frac{2\mu\nu}{\mu^2+\nu^2} = \tanh 2r, \quad S^{\rm cond}_{\hat{a}_{-\theta}\hat{a}_{-\theta}} = \frac{1}{\mu^2+\nu^2} = \frac{1}{\cosh 2r}. \tag{7}$$

In laser interferometer gravitational wave detectors, we have the input-output relation for quantum noise field in the signal channel as [2]:

$$\hat{A}_2 = e^{2i\beta}(\hat{a}_2 - \mathcal{K}\hat{a}_1) = e^{2i\beta}(\sqrt{1+\mathcal{K}^2})(\hat{a}_1\cos\xi - \hat{a}_2\sin\xi), \tag{8}$$

where $\hat{A}_2$ is the phase quadrature of the signal fields propagate out of the interferometer and $\xi = -\arctan 1/\mathcal{K}$. If we want the phase quadrature of the idler fields out of the interferometer $\hat{B}_2$ to maximally correlate with $\hat{A}_2$ in Eq. (8), then $\hat{B}_2 = \hat{b}_{\arctan 1/\mathcal{K}}$ (besides an unimportant phase factor α accumulated by sidebands of the idler field during its circulation in the interferometer). Therefore, the rotation angle of the idler field $\Phi_{\rm rot}$ by the interferometer defined in

$$\hat{B}_2 = e^{i\alpha}(-\hat{b}_1\sin\Phi_{\rm rot} + \hat{b}_2\cos\Phi_{\rm rot}), \tag{9}$$

is given as $\Phi_{\rm rot} = \arctan\mathcal{K}$.

Similarly, when combining the measurement results of signal and idler channel, we have:

$$\hat{A}^g_2 = \hat{A}_2 - g\hat{B}_2 \quad \text{and} \quad S_{\hat{A}^g_2\hat{A}^g_2} = S_{\hat{A}_2\hat{A}_2} + |g|^2 S_{\hat{B}_2\hat{B}_2} - g^* S_{\hat{A}_2\hat{B}_2} - g S_{\hat{B}_2\hat{A}_2}. \tag{10}$$

Variation with respect to filter gain factor g leads to the Wiener filter and a minimum variance given as:

$$g_{\rm opt} = \frac{S_{\hat{A}_2\hat{B}_2}}{S_{\hat{B}_2\hat{B}_2}} = e^{i(2\beta-\alpha)}\sqrt{1+\mathcal{K}^2}\tanh 2r, \tag{11}$$

$$S^{\rm cond}_{\hat{A}_2\hat{A}_2} = S_{\hat{A}_2\hat{A}_2} - \frac{S_{\hat{B}_2\hat{A}_2}S_{\hat{A}_2\hat{B}_2}}{S_{\hat{B}_2\hat{B}_2}} = \frac{1+\mathcal{K}^2}{\cosh 2r}. \tag{12}$$

Considering the signal field as: $\hat{A}^{\rm GW}_2 = \sqrt{2\mathcal{K}}e^{i\beta}h/h_{\rm SQL}$ [2], we can recover the Eq. (7) of the main text:

$$S_{\rm hh} = \frac{h^2_{\rm SQL}}{2\cosh 2r}\left(\mathcal{K} + \frac{1}{\mathcal{K}}\right). \tag{13}$$

II. PARAMETER SETTING

A. Requirements

Our conditional squeezing scheme is based on the combination of the results from signal beam detection and idler beam detection. If the squeezer's squeezing level is high, the parameter error will have a significant effect on the final squeezing level. For example, the effect of variation of the idler rotation angle to the sensitivity is roughly given by:

$$S_{\rm hh} = \frac{h^2_{\rm SQL}}{2\cosh 2r}\left(\mathcal{K} + \frac{1}{\mathcal{K}}\right) + \frac{h^2_{\rm SQL}}{2}\frac{(\sinh 2r)^2}{\cosh 2r}\left(\mathcal{K} + \frac{1}{\mathcal{K}}\right)\delta\Phi^2. \tag{14}$$

For a 15 dB squeezer as shown in the main text, the ratio between the correction term and the exact value is roughly $\approx 249\delta\Phi^2$. Therefore even a 10% relative correction to the noise spectrum requires the error of the rotation angle to be as small as 0.02 rad. This simple estimation tells us that it is of great importance to search the suitable parameters for our proposed scheme.

In our design, the signal field sees an interferometer working in the resonant sideband extraction mode while the idler field sees the interferometer as a filter cavity. This filter cavity should rotate the idler field in its phase space by an angle $\Phi_{\rm rot} = \arctan\mathcal{K}$. Generally, for realising such a rotation angle, two filter cavities are required [2] (for a

more general discussion, see [3]). However, when the signal field works in the resonant sideband extraction mode, the interferometer has a relatively large bandwidth so that $\mathcal{K}$ can be approximated around the transition frequency as: $\mathcal{K} \approx 2\Theta^3/(\Omega^2\gamma)$. In this case, only one filter cavity is necessary to achieve the required rotation of the idler field, and we use the signal recycling interferometer itself as the filter. The required bandwidth γ_f and detuning δ_f of the signal recycling interferometer with respect to the idler field is given by [3, 4]:

$$\gamma_f = \sqrt{\Theta^3/\gamma}, \quad \delta_f = -\gamma_f. \tag{15}$$

B. Parameter setting conditions

The dependence of detuning δ_f and bandwidth γ_f on the interferometer parameters can be seen in the interferometer reflectivity, which is given by (in the sideband picture) [5]:

$$r_{\rm ifo}^{\rm idler}(\Omega) = \frac{\rho + (\tau\tilde{\tau} - \rho\tilde{\rho})\exp[2i(\Delta+\Omega)L_{\rm arm}/c]}{1 - \tilde{\rho}\exp[2i(\Delta+\Omega)L_{\rm arm}/c]},; \tag{16}$$

where ρ, $\tilde{\rho}$, τ, and $\tilde{\tau}$ describe the reflectivity and transmissivity of the signal recycling cavity. They are given by [5]:

$$\begin{gathered}\tilde{\rho} = \frac{\sqrt{R_{\rm ITM}} - \sqrt{R_{\rm SRM}}\exp[2i\phi_{\rm SRC}]}{1 - \sqrt{R_{\rm ITM}R_{\rm SRM}}\exp[2i\phi_{\rm SRC}]}, \quad \rho = -\frac{\sqrt{R_{\rm SRM}} - \sqrt{R_{\rm ITM}}\exp[2i\phi_{\rm SRC}]}{1 - \sqrt{R_{\rm ITM}R_{\rm SRM}}\exp[2i\phi_{\rm SRC}]}, \\ \tau = \tilde{\tau} = \frac{i\sqrt{T_{\rm SRM}\sqrt{T_{\rm ITM}}}\exp[i\phi_{\rm SRC}]}{1 - \sqrt{R_{\rm SRM}R_{\rm ITM}}\exp[2i\phi_{\rm SRC}]}.\end{gathered} \tag{17}$$

Here, $R_{\rm ITM}$ and $R_{\rm SRM}$ are the power reflectivity of the input test mass mirrors and the signal recycling mirror, respectively. The $\phi_{\rm SRC}$ is the single trip phase of the idler field in the signal recycling cavity given as:

$$\phi_{\rm SRC} = \Delta L_{\rm SRC}/c. \tag{18}$$

From Eq.(16), the resonance condition can be derived as:

$$\boxed{\mathrm{Mod}_{2\pi}\left[2(\delta_f + \Delta)\left(\frac{L_{\rm arm}}{c}\right) + \mathrm{Arg}[\tilde{\rho}]\right] = 0,} \tag{19}$$

which determines the detuning δ_f. The bandwidth γ_f is given by:

$$\boxed{\gamma_f \approx \frac{T_{\rm SRM}}{1 + R_{\rm SRM} + 2\sqrt{R_{\rm SRM}}\cos 2\phi_{\rm SRC}}\gamma_{\rm ITM},} \tag{20}$$

where $\gamma_{\rm ITM} = cT_{\rm ITM}/(4L_{\rm arm})$.

From Eq.(19) and (20), when the reflectivity of the signal recycling mirror and the input test mass mirror is given, we have the following tunable parameters: (1) detuning of the idler beam with respect to the signal beam Δ, (2) arm cavity length $L_{\rm arm}$, (3) the phase $\phi_{\rm SRC}$. These parameters must be tuned in such a way so that arm cavity and signal recycling cavity must each be resonant with the signal carrier frequency ω_0 for keeping the signal channel unaffected. This means that the length tuning of the signal recycling cavity and the arm cavities (denoted by $\delta L_{\rm arm}$ and $\delta L_{\rm SRC}$, respectively) , starting from their initial lengths (denoted by $L_{\rm arm}^{(0)}$ and $L_{\rm SRC}^{(0)}$, respectively) should be integer numbers of half wavelength of the main carrier field, that is

$$\delta L_{\rm SRC} = p\lambda/2, \quad \delta L_{\rm arm} = q\lambda/2, \quad (p, q \in \mathbb{Z}). \tag{21}$$

Also note that Eq.(15) tells us that γ_f and δ_f depends on $\delta L_{\rm arm}$ while not on $\delta L_{\rm SRC}$. Since $L_{\rm arm}^{(0)}$ is typically of kilometer scale, thereby $\delta L_{\rm arm}$ as a small length tuning has negligible effect on the value of required γ_f and δ_f.

To obtain the required bandwidth γ_f, we can tune the $\phi_{\rm SRC}$ by tuning Δ and $L_{\rm SRC}$ in Eq.(18) to satisfy:

$$\phi_{\rm SRC} = \Delta L_{\rm SRC}/c = \frac{1}{2}\arccos\left[\frac{\gamma_{\rm ITM}}{\gamma_f}T_{\rm SRM} - (1 + R_{\rm SRM})\right] + n\pi, \tag{22}$$

or in another form:

$$\Delta = \frac{c}{2L_{\rm SRC}} \arccos\left[\frac{\gamma_{\rm ITM}}{\gamma_f} T_{\rm SRM} - (1 + R_{\rm SRM})\right] + \frac{n\pi c}{L_{\rm SRC}}, \tag{23}$$

which tells us that n, as a tunable degree of freedom, represents how many free-spectral range of signal recycling cavity contained by the idler detuning Δ. In summary, we have three tunable integers: m, n and p. For a fixed value of n, the phase $\phi_{\rm SRC}$ only depends on the $L_{\rm SRC} = L_{\rm SRC}^{(0)} + p\lambda/2$, thus the rough range of p can be determined. To obtain the required detuning δ_f, we need to further do fine tuning of p and then do a corresponding tuning of q to match the resonance condition Eq.(19). A sample parameter set is given in Tab. I. We also need to emphasise that the practical parameters setting should be decided considering concrete experimental requirements, and a feedback control system for length tuning needs to be carefully designed, what we have here is merely an example demonstrating that these parameters can in principle be found.

C. Phase compensation

Note that since the detuned $\hat{b}-$ field will pick up a phase when it is reflected by the signal recycling cavity, which will contribute an additional rotation angle, we need to compensate this phase by properly choosing the homodyne angle. This fact can be seen by manipulating(16), given as follows.

From Eq. (17), we can derive the following relation:

$$\frac{\tilde{\rho}^*}{\rho} = -\frac{1}{\tau^2 - \rho\tilde{\rho}}. \tag{24}$$

Substituting this relation into Eq.(16) leads to:

$$\begin{aligned} r_{\rm ifo}^{\rm idler}(\Omega) &= \frac{-\tilde{\rho}^*(\tau^2 - \rho\tilde{\rho}) + (\tau^2 - \rho\tilde{\rho})\exp[2i(\Delta+\Omega)L_{\rm arm}/c]}{1 - \tilde{\rho}\exp[2i(\Delta+\Omega)L_{\rm arm}/c]} \\ &= \left[\frac{-\tilde{\rho}^* + \exp[2i(\Delta+\Omega)L_{\rm arm}/c]}{1 - \tilde{\rho}\exp[2i(\Delta+\Omega)L_{\rm arm}/c]}\right](\tau^2 - \rho\tilde{\rho}). \end{aligned} \tag{25}$$

Note that $\tilde{\rho} = |\tilde{\rho}|e^{i{\rm Arg}[\rho]}$ and $|\tau^2 - \rho\tilde{\rho}| = 1$, therefore the above $r_{\rm ifo}^{\rm idler}$ can be written as:

$$r_{\rm ifo}^{\rm idler} = \left[\frac{-|\tilde{\rho}| + \exp[2i(\Delta+\Omega)L_{\rm arm}/c + i{\rm Arg}[\tilde{\rho}]]}{1 - |\tilde{\rho}|\exp[2i(\Delta+\Omega)L_{\rm arm}/c + i{\rm Arg}[\tilde{\rho}]]}\right] e^{i\phi_c}, \tag{26}$$

where

$$\phi_c = {\rm Arg}\left[\tau^2 - \rho\tilde{\rho}\right] - {\rm Arg}[\tilde{\rho}]. \tag{27}$$

Since $\Omega L_{\rm SRC}/c \ll 1$, the ϕ_c dependence on Ω is very weak. Therefore this additional phase can be treated as almost a D-C phase. In our sample example, for compensating this additional phase angle, the phase of the homodyne detector of idler channel must be tuned by $\phi_c = 0.32$ rads.

D. A sample rotation angle

Using the parameters given in Tab. I, we are able to produce the frequency dependent rotation angle for the $\hat{b}-$fields measured by the homodyne detector with local oscillator frequency $\omega_0+\Delta$, as shown in Fig. 1. This figure demonstrates that the proposed parameters in Tab. I lead to a result that is very close to the required rotation angle. The angle error is also given in the right panel of Fig. 1, which shows that our result has maximally 0.04 rads angle error in the intermediate frequency band (50-300 Hz), creates a 40% relative correction to the noise spectrum according to our estimation formula Eq. (14), degrading the improvement factor from 12 dB to 10.5 dB. Exact computation shows that the degraded improvement factor is around 11.1 dB.

λ	carrier laser wavelength	1064nm
$T_{\rm SRM}$	SRM power transmissivity	0.35
T	ITM power transmissivity	0.014
$L_{\rm arm}^{(0)}$	Arm cavity initial length	4km[1]
$L_{\rm SRC}^{(0)}$	Signal recycling cavity initial length	50m[1]
γ	Detection bandwidth	389 Hz
m	Mirror mass (ITM and ETM)	40kg
I_c	Intra cavity power	650kW
Δ	Idler detuning	-300 kHz-5FSR$_{SRC}$(=-15.3 MHz)
r	Squeezing factor of the OPA	1.23 (15dB)
$\delta L_{\rm arm}$	Arm length tuning	19850λ
$\delta L_{\rm src}$	SRC length tuning	26λ
ϕ_c	Phase compensation	0.32 rads

[1] These numbers are approximated value since the exact length should be integer number of half wavelength since both the arm cavity and signal recycling cavity should be on resonance with the main carrier light. In particular, the exact length of arm cavity closest to 4 km is 3759398496λ; for exact length of signal recycling cavity closest to 50 m is 46992481λ.

TABLE I: Sample Parameters for implementing our scheme on the Advanced LIGO. Here $\mathrm{FSR}_{\rm SRC} = c/(2L_{\rm SRC})$.

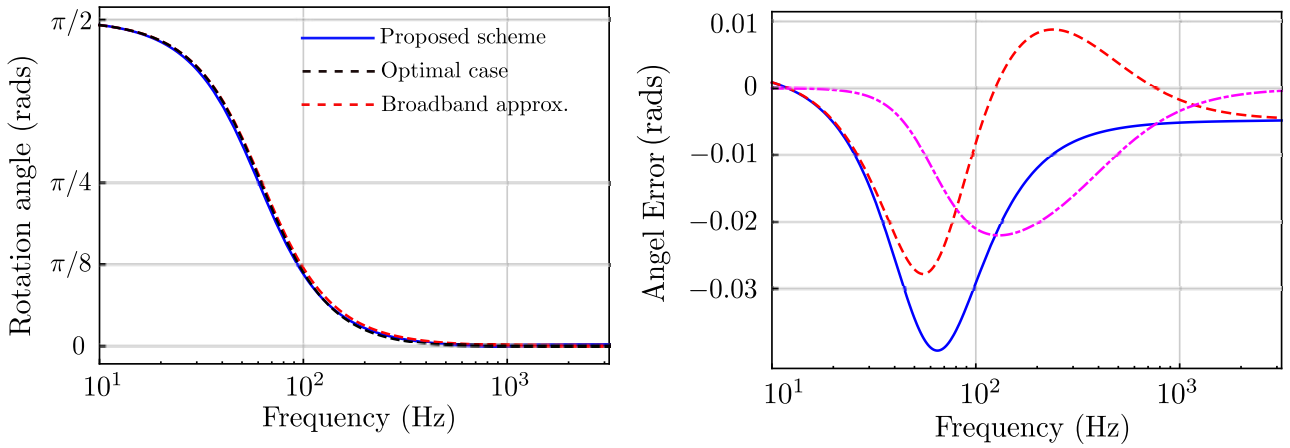

FIG. 1: Left panel: Rotation angle for the $\hat{b}-$ field. The blue curve is the result computed using the parameters given in Tab.1 of the main text and exact transfer matrix technique. The red dashed curve is the optimal result of $\Phi_{\rm rot} = -\arctan\mathcal{K}$ while the black dashed curve is the rotation angle when we approximate $\mathcal{K}$ using broadband approximation as discussed in the main text of this supplementary material. Right panel: Error of the rotation angle. (1)The magenta dotdashed curve is the difference between the analytical result of rotation angle under broadband approximation and the optimal angle ; (2) the blue curve is the difference between the rotation angle computed from our proposed scheme and the analytical result under broadband approximation; (3) the red dashed curve is the difference between the rotation angle computed from our proposed scheme and the optimal analytical result.

III. LOSS ANALYSIS

Fig.3 of the main text takes into account of the loss in our system. There are four main loss sources in our design: (1) the loss due to the arm cavity and signal recycling cavity, which currently has the value round 100 ppm (per round trip) and 2000 ppm (per round trip) and has a relatively small effect on the sensitivity, compare to the current filter cavity design which has the value around 1ppm per meter. (2) the input loss comes from the loss of the optical devices in the input optical path and mode mismatch; the readout loss comes from the measurement channel due to the non-perfect quantum efficiency of the photo-detector, the lossy optical devices in the output optical path and also mode mismatch. (3) The phase fluctuation of the local oscillators which are used to measure the $\hat{a}$ and $\hat{b}-$fields.

A. Arm cavity loss and signal recycling cavity loss

Similar to what has been discussed in [6], for the signal channel, 100 ppm round trip loss in the arm cavity corresponds to about 0.3% total loss (considering the circulation of light fields) in advanced LIGO since it works in the resonant sideband extraction mode, which is comparable to the impact of signal recycling cavity loss ($\sim 0.2\%$) at the interesting frequency band. However, since the large detuned idler field does not resonant with the signal recycling cavity, thereby a more careful simulation is needed. We simulate the effects of these noises in the following Fig. 2 to compare the impact of these different noise sources (a similar figure was also shown in [6]). Note that at low frequency, the impact of these noises on the idler channel is much less than that on the signal channel, since the idler field does not drive the interferometer mirrors through random radiation pressure force noise in the interested frequency domain.

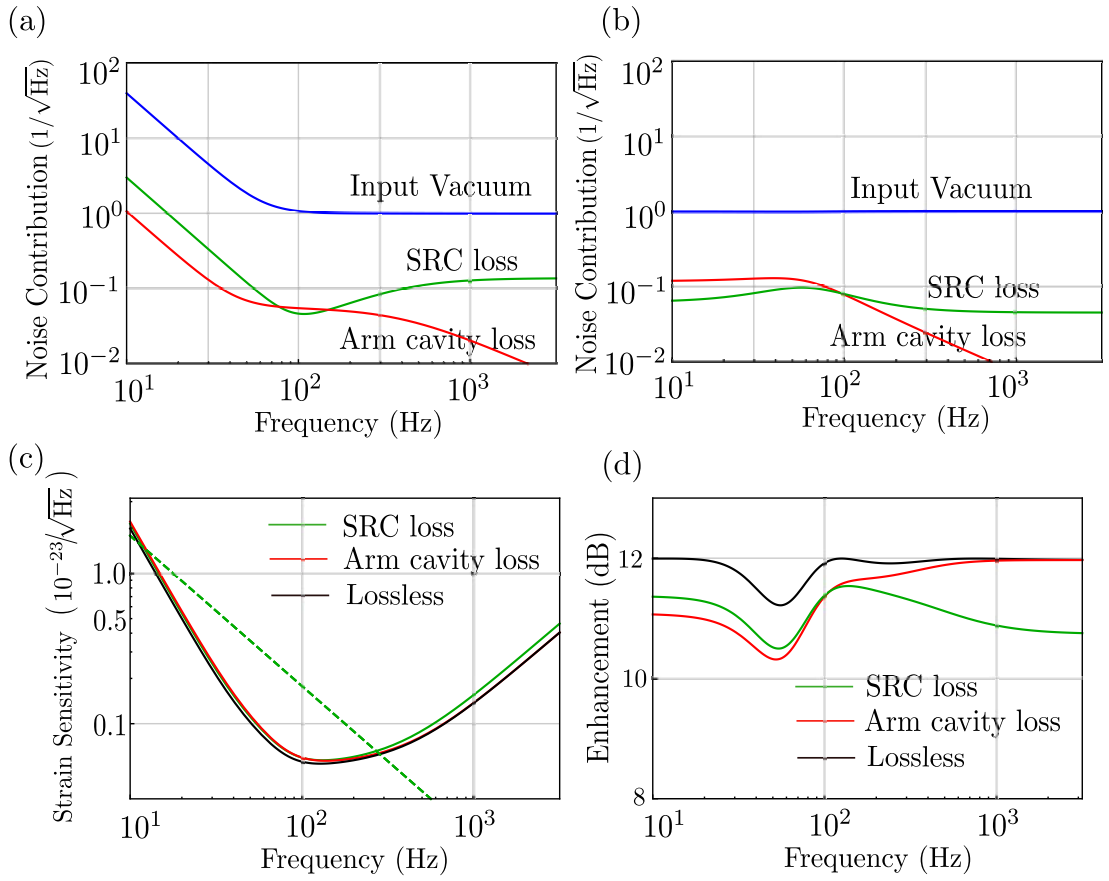

FIG. 2: Simulation of quantum noise contributions from the arm and signal recycling cavities (round trip losses $\epsilon_c = 100$ ppm and $\epsilon_{\rm SRC} = 2000$ ppm respectively, as in the main text) and their impact on strain sensitivity and sensitivity enhancement. (a) Signal channel: comparison of quantum noise contributions in the signal channel from (unsqueezed) vacuum fluctuations, arm cavity loss, and SRC loss. The noise fields beat with a strong carrier field, resulting in radiation pressure noise below 50 Hz due to the ponderomotive effect. (b) Idler channel: comparison of contributions in the idler channel from (unsqueezed) vacuum fluctuations, arm cavity loss and SRC loss. The noise fields do not beat with the strong carrier field, and therefore do not participate in the ponderomotive process. (c) The (small) impact of loss due to combined signal and idler channels, shown separately for arm cavity loss and SRC loss (d) Impact of cavity losses on sensitivity enhancement factor for the proposed conditioning scheme.

B. Input Loss and readout loss

Let us now investigate the effect of the input loss and the readout loss. The sensitivity curve in Fig. 3 of the main text is computed using numerical transfer-matrix approach [8]. Here for giving an analytical formula, we apply the

single-mode approximation which is a very good approximation within one free-spectral-range of the arm cavity. The exact results about the contribution from the input loss and readout loss respectively are shown in Fig. 3. Since the $\hat{a}$ and $\hat{b}$ fields propagate in a collinear way and share the same optical mode, therefore the input and readout loss of the $\hat{a}$ and $\hat{b}-$fields are the same, denoted by $\epsilon_{\rm in}$ (in terms of power) and we have:

$$\hat{a} \to \sqrt{1-\epsilon_{\rm in}}\hat{a} + \sqrt{\epsilon_{\rm in}}\hat{n}_s^{\rm in}, \quad \hat{b} \to \sqrt{1-\epsilon_{\rm in}}\hat{b} + \sqrt{\epsilon_{\rm in}}\hat{n}_i^{\rm in}, \tag{28}$$

$$\hat{A}_2 \to \sqrt{1-\epsilon_r}\hat{A}_2 + \sqrt{\epsilon_r}\hat{n}_s^r, \quad \hat{B}_2 \to \sqrt{1-\epsilon_r}\hat{B}_2 + \sqrt{\epsilon_r}\hat{n}_i^r. \tag{29}$$

where $\hat{n}_s^{\rm in}$ and $\hat{n}_i^{\rm in}$ are two uncorrelated injection noises and $\hat{n}_s^r$ and $\hat{n}_i^r$ are two uncorrelated readout noises associated with two homodyne detectors.

Expand to the first order of $\epsilon_{\rm in}$ and ϵ_r, we have the approximated formula for the degradation of the strain sensitivity as a summation of input loss contribution $\Delta S_{\rm hh}^{\epsilon_{\rm in}{\rm cond}}$ and the readout loss contribution $\Delta S_{\rm hh}^{\epsilon_r{\rm cond}}$:

$$\Delta S_{\rm hh}^{\epsilon{\rm cond}} = \Delta S_{\rm hh}^{\epsilon_{\rm in}{\rm cond}} + \Delta S_{\rm hh}^{\epsilon_r{\rm cond}} \tag{30}$$

where:

$$\Delta S_{\rm hh}^{\epsilon_{\rm in}{\rm cond}} \approx \frac{h_{\rm SQL}^2}{2\cosh 2r}\left(\mathcal{K}+\frac{1}{\mathcal{K}}\right)\left(\frac{2\cosh 2r^2 - \cosh 2r - 1}{\cosh 2r}\right)\epsilon_{\rm in} \tag{31}$$

$$\Delta S_{\rm hh}^{\epsilon_r{\rm cond}} \approx \frac{h_{\rm SQL}^2}{2}\left(\mathcal{K}\tanh^2 2r + \frac{1+\tanh^2 2r}{\mathcal{K}}\right)\epsilon_r. \tag{32}$$

$$\tag{33}$$

It is easy to see that the effect of the input loss contributes a broadband degradation of squeezing degree. This degradation is frequency independent. However, for the readout loss, at high frequencies where $\mathcal{K} \ll 1$ the relative loss correction is roughly $\Delta S_{\rm hh}^{\epsilon_r{\rm cond}}/S_{\rm hh}^{\rm cond} \approx [1+(\tanh 2r)^2]\epsilon_r$, while at low frequencies where $\mathcal{K} \gg 1$, $\Delta S_{\rm hh}^{\epsilon_r{\rm cond}}/S_{\rm hh}^{\rm cond}$ is roughly $(\tanh 2r)^2\epsilon_r$. Therefore the readout loss effect at high frequencies is higher than that at low frequencies, due to the fact that the pondermotive effect amplifies the signal at the low frequency band [2]. This character of the sensitivity curves has been shown in Fig. 3 of the main text and more explicitly in Fig. 3 of this Supplementary Material.

If we take the assumption of $\epsilon_{\rm in} = \epsilon_r = \epsilon$, the noise spectrum for the traditional broadband squeezing using an additional filter cavity and the conditional squeezing, including the loss ϵ to the first order, and under the approximation that the squeezing degree is large, we have:

$$\Delta S_{\rm hh}^{\epsilon{\rm cond}} \approx \frac{h_{\rm SQL}^2}{2}\left(\frac{2}{\mathcal{K}}+\frac{3}{2}\mathcal{K}\right)2\epsilon, \quad \Delta S_{\rm hh}^{\epsilon{\rm tran}} \approx \frac{h_{\rm SQL}^2}{2}\left(\frac{2}{\mathcal{K}}+\mathcal{K}\right)\epsilon, \tag{34}$$

where $\Delta S_{\rm hh}^{\epsilon{\rm tran}}$ is the first order correction to the sensitivity curve produced by traditional squeezing scheme [2, 7] and clearly we have $\Delta S_{\rm hh}^{\epsilon{\rm cond}} \approx 2\Delta S_{\rm hh}^{\epsilon{\rm tran}}$. As we have briefly mentioned in the main text, due to the fact that both signal and idler beams experience the same loss during their propagation in our scheme, the input and readout losses in our configuration are roughly doubled compare to that of the traditional squeezing scheme with an additional filter cavity.

C. Phase fluctuation

The classical phase uncertainty of local oscillators in homodyne detection scheme has a very small effect on the sensitivity, proved as follows.

We assume that the phase fluctuation of the local oscillators used for signal and idler detection are independent Gaussian random variables represented by ξ_s and ξ_i respectively, with zero mean and standard variacne ξ_{vs} and ξ_{vi}, such that their probability density functions are given by:

$$P_s(\xi_s) = \frac{1}{\sqrt{2\pi\xi_{vs}^2}}e^{-\frac{\xi_s^2}{2\xi_{vs}^2}}, \quad P_i(\xi_i) = \frac{1}{\sqrt{2\pi\xi_{vi}^2}}e^{-\frac{\xi_i^2}{2\xi_{vi}^2}}, \tag{35}$$

For measuring any field $\hat{O}$, the effect of phase fluctuation ξ_O in a phase quadrature readout scheme is that the actual detected quadrature is also a random variable which is given by $\hat{O}_m(t) = -\hat{O}_1(t)\sin\xi_O + \hat{O}_2(t)\cos\xi_O$. The

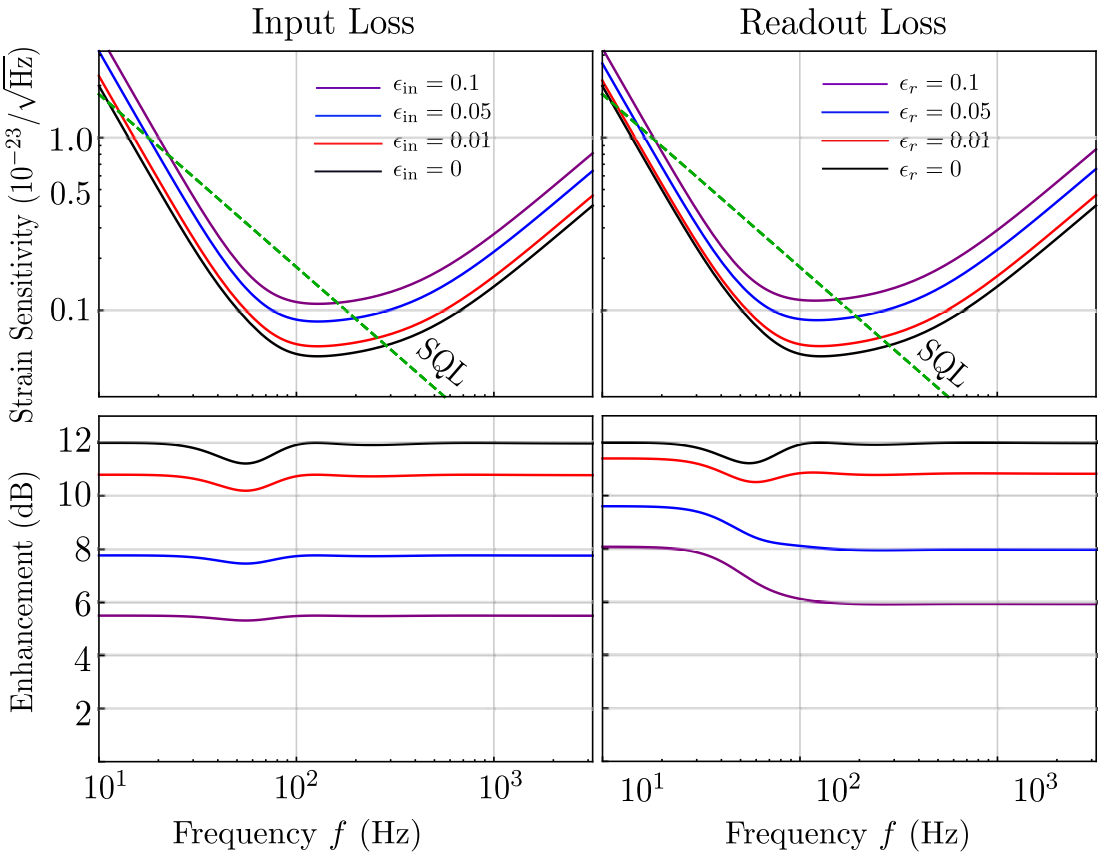

FIG. 3: Left panel: the strain sensitivity and enhancement factor of our configuration when there is only input loss. Right panel: the strain sensitivity and enhancement factor of our configuration when there is only readout loss.

ensemble-averaged variance of the detected quadrature is then [9]:

$$\begin{aligned} S_{\hat{O}_m\hat{O}_m} &= \frac{1}{2}\int d\xi_O P(\xi_O)\langle \hat{O}_m\hat{O}_m^\dagger + \hat{O}_m^\dagger\hat{O}_m\rangle \\ &= V_{\hat{O}_1\hat{O}_1}\int d\xi_O P(\xi_O)\sin\xi_O^2 + V_{\hat{O}_2\hat{O}_2}\int d\xi_O P(\xi_O)\cos\xi_O^2 + (V_{\hat{O}_1\hat{O}_2} + V_{\hat{O}_2\hat{O}_1})\sin\xi_O\cos\xi_O \end{aligned} \tag{36}$$

Now if we use the identities (we assume that $\xi_{vo} \ll 1$.):

$$\begin{aligned} \int d\xi_O P(\xi_O)\sin^2\xi_O &= e^{-\xi_{ov}^2}\sinh\xi_{ov}^2 \approx \xi_{ov}^2 \approx \sin\xi_{ov}^2 \\ \int d\xi_O P(\xi_O)\cos^2\xi_O &= e^{-\xi_{ov}^2}\cosh\xi_{ov}^2 \approx 1-\xi_{ov}^2 \approx \cos\xi_{ov}^2, \end{aligned} \tag{37}$$

and the fact that the $\sin\xi_O\cos\xi_O$ is an odd function, one can obtain:

$$S_{\hat{O}_m\hat{O}_m} \approx \cos\xi_{vo}^2 V_{\hat{O}_1\hat{O}_1} + \sin\xi_{vo}^2 V_{\hat{O}_2\hat{O}_2}. \tag{38}$$

Using the above formula, one can can compute the variance of signal and idler fields.

Similarly, the cross correlation between the signal and idler fields (represented by $\hat{A}$ and $\hat{B}$) in the phase quadrature readout scheme, accounting for phase fluctuations, is given by:

$$S_{A_mB_m} = \frac{1}{2}\int d\xi_i d\xi_s P(\xi_i)P(\xi_s)\langle(\hat{A}_1\sin\xi_s + \hat{A}_2\cos\xi_s)(\hat{B}_1\cos\xi_i + \hat{B}_2\sin\xi_i)\rangle. \tag{39}$$

Because ξ_i and ξ_s are two independent random variables, the above cross correlation fluctuation leads to:

$$S_{A_mB_m} = S_{A_2B_1}e^{-\frac{\xi_{vs}^2+\xi_{vi}^2}{2}} \approx S_{a_2b_1}\left(1-\frac{\xi_{vs}^2+\xi_{vi}^2}{2}\right). \tag{40}$$

where we have used the identities:

$$\int d\xi_O P(\xi_O)\cos\xi_O = e^{-\frac{\xi_O^2}{2}}, \quad \int d\xi_O P(\xi_O)\sin\xi_O = 0. \tag{41}$$

Substituting Eq. (38) and Eq. (40) into Eq. (11), the final strain sensitivity can be written as:

$$S_{hh} = \frac{h_{\mathrm{SQL}}^2}{2\cosh 2r}\left[\frac{1+(\xi_{vs}^2+\xi_{vi}^2)\sinh 4r}{\mathcal{K}} + (1-\xi_{vs}^2+\xi_{vi}^2\sinh 4r)\mathcal{K}\right]. \tag{42}$$

The typical experimental rms of the local oscillator phase is taken to be 1.7m rad such as shown in [10], that means the phase fluctuation quantities in the above formula have an orders of magnitude $\sim 10^{-6}$ rad^2. For a 15dB squeezer, 1 mrad phase jittering only contributes roughly $\sim 0.5\%$ relative correction to the final sensitivity.

[1] M. O. Scully and M. S. Zubairy. *Quantum Optics (Chapter 16)*. Cambridge University Press, 1997.

[2] H. J. Kimble, Yu. Levin, A. B. Matsko, K. S. Thorne, and S. P. Vyatchanin. Conversion of conventional gravitational-wave interferometers into quantum nondemolition interferometers by modifying their input and/or output optics. *Phys. Rev. D*, 65(022002), 2001.

[3] P. Purdue and Y. Chen. Practical speed meter designs for quantum nondemolition gravitational-wave interferometers. *Phys. Rev. D*, 66(122004), 2002.

[4] F. Ya. Khalili. Quantum variational measurement in the next generation gravitational-wave detectors. *Phys. Rev. D*, 76(102002), 2007.

[5] A. Buonanno and Y. Chen. Scaling law in signal recycled laser-interferometer gravitational-wave detectors. *Phys. Rev. D*, 67(062002), 2003.

[6] L. Barsotti. Squeezing for Advanced LIGO. *LIGO Document*, G1401092-v1, 2014.

[7] H. Miao, H. Yang, R. X. Adhikari, and Y. Chen. Quantum limits of interferometer topologies for gravitational radiation detection. *Classical Quantum Gravity*, 31(16), August 2014.

[8] T. Corbitt, Y. Chen, and N. Mavalvala. Mathematical framework for simulation of quantum fields in complex interferometers using the two-photon formalism. *Phys. Rev. A*, 72(013818), July 2005.

[9] T. Aoki, G. Takahashi, and A Furusawa. Squeezing at 946nm with periodically poled KTiOPO4. *Opt. Express*, 14(15):6930–6935, 2006.

[10] Vahlbruch, H., Mehmet, M., Danzmann, K., and Schnabel, R. Detection of 15 dB squeezed states of light and their application for the absolute calibration of photo-electric quantum efficiency. *Physical Review Letters*, **117** (110801), (2016).